One-dimensional hydrodynamic model accounting for tidal effect

Xiaoqin Zhang, Weimin Bao, Simin Qu and Zhongbo Yu

ABSTRACT

Tidal effect has a significant impact on flood routing in tidal rivers, conceptually taking on a resistant effect during flood tide and a dynamic effect during ebb tide. Two expressions were developed to reflect the tidal effect in this study, which consisted of the tidal wave velocity, the change rate of tidal level and the change in channel width. By incorporating the expressions into the momentum equation of the one-dimensional (1D) Saint-Venant equations, we propose that there are two types of momentum equations accounting for tidal effect. Based on the continuity equation and proposed momentum equations, two types of 1D hydrodynamic model for tidal rivers (namely the SVN-1 and -2 models) were constructed. In the case study, these models were applied to the tidal reach of the Qiantang River in China. The simulation results show that the SVN-1 and -2 models can obtain better accuracy than the SVN model based on the standard Saint-Venant equations, and that the SVN-1 model performs better than the SVN-2 model. Furthermore, the SVN-1 model can effectively capture water-level fluctuation, indicating that the expression employed is capable of accounting for tidal effect.

Key words | 1D hydrodynamic model, channel geometry, flood routing, tidal effect, tidal river

Xiaoqin Zhang (corresponding author)
Weimin Bao
Simin Qu
Zhongbo Yu
State Key Laboratory of Hydrology-Water Resources and Hydraulic Engineering,
College of Hydrology and Water Resources,
Hohai University,
Nanjing 210098,
China
E-mail: *zxqin403@163.com*

Zhongbo Yu
Department of Geoscience,
University of Nevada Las Vegas,
NV 89154,
USA

INTRODUCTION

Hydrodynamic processes are manifestly complex in tidal rivers. Flow in a tidal river is composed of contributions from the upstream flood and the downstream tide. Consequently, inundations due to the coincidence of river floods and tides are a potential source of damage. It is known that tidal effect has a profound influence on river flood routing, sediment transport and estuary ecology. The hydrologic systems in open-channel flows under tidal effect are unique with periodic changes in water level and velocity. It is difficult to forecast tidal river flow movement involving bidirectional wave propagation in the opposite directions.

Traditional flood forecasting methods accommodating tidal effect, such as the corresponding stage method which focuses on peak stages and the conversion method based on a rating curve, have been used for decades. Three types of approaches for flood forecasting in tidal rivers have been developed, including hydrologic models based on empirical storage–flow relations to approximate momentum effects (e.g. Bao *et al.* 2007; Qu *et al.* 2009), mathematical models based on data analysis (e.g. Chang & Chen 2003; Yu *et al.* 2006) and hydrodynamic models based on hydrodynamic equations (e.g. Liu *et al.* 2007; Lei *et al.* 2009). Compared with hydrologic models and mathematical models, hydrodynamic models are physically based, which can describe the dynamic mechanism of unsteady flow. Due to ease of use with respect to higher-dimensional models, the one-dimensional (1D) hydrodynamic models based on the standard Saint-Venant equations (the SVN model) have been widely used for numerical simulation of water flow in tidal rivers (e.g. Su *et al.* 2001; Saavedra *et al.* 2003; Hsu *et al.* 2006).

Tide propagation can produce a downstream backwater effect, resulting in significant impacts on flood routing. Although flood wave propagation has been studied extensively (e.g. Ferrick 1985; Tayefi *et al.* 2007; Price 2009), the tidal effect on flood routing remains an important subject for further study. The presence of the downstream backwater condition in channel flow can rebalance the gravity,

doi: 10.2166/nh.2011.114

friction, water pressure and other forces, leading to the adjustment of the wave attenuation characteristics (Tsai 2003, 2005). Likewise, river discharge has a considerable influence on tide propagation (e.g. Horrevoets *et al.* 2004). It is known that the downstream boundary condition can represent the backwater effect to some extent. However, in the derivation of the Saint-Venant equations, no attention has been directly paid to the tidal effect. Performance of the hydrodynamic models based on the Saint-Venant equations is generally unsatisfactory when applied to rivers with significant tidal effect.

The question of how to effectively consider the tidal effect on flood routing therefore arises. It is known that tide propagation is significantly affected by channel geometry and tidal characteristics. In concept, the longer the distance from a specific section to the channel mouth in a tidal channel, the smaller the tidal effect on flood routing at the section. In terms of the characteristics of tide propagation, the approach of adding an expression into the momentum equation of the standard Saint-Venant equations is proposed to account for tidal effect. Further, two types of 1D hydrodynamic models based on the modified Saint-Venant equations for tidal rivers, referred to as the SVN-1 and -2 models, are constructed. The performances of the SVN-1 model, the SVN-2 model and the original SVN model are compared using a case study.

METHODOLOGY

Saint-Venant equations

The governing equations of the standard Saint-Venant equations representing 1D flow movement in a wide open channel can be expressed as:

$$B\frac{\partial h}{\partial t}+\frac{\partial(Av)}{\partial x}=0 \tag{1}$$

$$\frac{\partial v}{\partial t}+v\frac{\partial v}{\partial x}+g\frac{\partial h}{\partial x}+\frac{gv|v|}{c^2R}=gS_0 \tag{2}$$

where S_0 is the riverbed gradient, h is the water depth, B is the channel width, A is the cross-section area, g is the gravitational acceleration, x is the longitudinal distance, v is the flow velocity, t is the time, R is the hydraulic radius and c is the Chezy coefficient. Equation (1) is the continuity equation and Equation (2) is the momentum equation.

Tidal effect

Tide originates in open seas downstream of waterways where shallow open-channel waves emanate and travel upstream. Tidal effect has a great impact on flood routing. Mechanically, tidal effect can be simply regarded as a kind of horizontal stress action on a water body, which conceptually takes on a resistant effect in flood tide process and a dynamic effect in ebb tide process.

Tidal effect varies with estuary geometry, tidal wave reflection and bed friction. Tide periodically propagates upstream or downstream with the change in tidal wave energy. It is known that the tidal wave energy is closely related to tidal range, and tidal range is greatly affected by river geometry and bottom friction. River geometry may cause the tidal range to increase or decrease (as the river cross-section contracts or expands). Friction and reflection can dissipate tidal energy and reduce the tidal range as the tide propagates upstream.

Bidirectional flows occur in tidal rivers involving flood moving downstream and tide periodically propagating upstream or downstream. The transition of propagation direction upstream or downstream may be changed with the variability controlled not only by the relative magnitude of upstream inflow and tidal effect, but also by channel geometry as well as initial and boundary conditions (Phillips & Slattery 2007). Moreover, the channel geometric characteristics vary spatially and temporally, which may make the direction transition more complicated.

Tide propagation is the dominant mechanism controlling water surface elevation in the reach close to channel mouth, except in the condition that the effect of incoming flood exceeds that of downstream tide when upstream discharge extends its influence to the channel mouth in large floods. Conceptually, the longer the distance from a specific station to the downstream boundary in a tidal river, the smaller will be tidal effect on flood routing at the specific station. Generally, the larger the velocity at which the tidal

wave propagates, the greater the effect of the tide on flood routing.

Based on the analysis above, it is conceptually reasonable to express the tidal effect on flood routing at a specific section in a tidal river as the combined effect of the geometric changes in river channel, the change rate of tidal level at the downstream boundary, the tidal wave velocity and the distance from the specific station to the downstream boundary. Considering that it is difficult to completely use the channel geometry data along a river, river channel widths according to water levels were adopted to simply reflect the spatial and temporal change in channel section shapes. In light of the combination of these factors, two expressions were developed to reflect the comprehensive effect of tide:

$$\alpha\frac{B_T}{B_x}\omega\left|\frac{\partial T}{\partial t}\right|$$

and

$$\alpha\frac{B_T}{B_x}|\omega|\frac{\partial T}{\partial t}$$

where α is the kinetic energy coefficient of tidal wave, ω is the wave velocity, B_T is the channel width at the downstream boundary according to tidal level, B_x is the channel width at the cross-section according to river stage, the subscript x represents the length from the specific section to the downstream boundary, and T is the downstream tidal level. B_T/B_x is adopted to represent the change in channel geometry, and $\partial T/\partial t$ is used to show the change rate of tidal level at the downstream boundary.

Assume that the positive direction is from upstream to downstream. By incorporating the above two expression into Equation (2), we have:

$$\frac{\partial v}{\partial t}+v\frac{\partial v}{\partial x}+g\frac{\partial h}{\partial x}+\frac{gv|v|}{c^2R}-\alpha\frac{B_T}{B_x}\omega\left|\frac{\partial T}{\partial t}\right|=gS_0 \tag{3}$$

and

$$\frac{\partial v}{\partial t}+v\frac{\partial v}{\partial x}+g\frac{\partial h}{\partial x}+\frac{gv|v|}{c^2R}+\alpha\frac{B_T}{B_x}|\omega|\frac{\partial T}{\partial t}=gS_0 \tag{4}$$

From Equation (3), the direction of ω is upstream and takes a negative value during the flood tide process, thus:

$$-\alpha\frac{B_T}{B_x}\omega\left|\frac{\partial T}{\partial t}\right|$$

where a positive value represents the resistant effect. When the direction of ω is downstream with positive value in ebb tide process, we have:

$$-\alpha\frac{B_T}{B_x}\omega\left|\frac{\partial T}{\partial t}\right|$$

which represents dynamic effect when negative.

From Equation (4), $\alpha(B_T/B_x)|\omega|(\partial T/\partial t)$represents the resistant effect during a flood tide when positive, and the dynamic effect during an ebb tide when negative.

When $\alpha=0$, Equations (3) and (4) are equivalent to Equation (2). Equations (1) and (3) are employed to construct the SVN-1 model and Equations (1) and (4) are combined to establish the SVN-2 model (both 1D). Conceptually, both the SVN-1 and -2 models represent tidal effect. However, whether their performances are consistent with the conceptual analysis remains to be verified. The case study in the following section analysed the performance of the original SVN model and the SVN-1 and -2 models when applied to tidal rivers.

Difference solution

The governing equations involved in these models are discretized by using the classic four-point implicit difference Preissmann scheme:

$$\begin{cases} f(x,t)=\dfrac{\theta}{2}(f_{j+1}^{i+1}+f_j^{i+1})+\dfrac{1-\theta}{2}(f_{j+1}^{i}+f_j^{i}) \\ \dfrac{\partial f}{\partial x}=\theta\dfrac{f_{j+1}^{i+1}-f_j^{i+1}}{\Delta x}+(1-\theta)\dfrac{f_{j+1}^{i}-f_j^{i}}{\Delta x} \\ \dfrac{\partial f}{\partial t}=\dfrac{f_{j+1}^{i+1}-f_{j+1}^{i}+f_j^{i+1}-f_j^{i}}{2\Delta t} \end{cases} \tag{5}$$

where the subscripts j and $j+1$ represent space-discrete, the superscripts i and $i+1$ represent time-discrete, f is a variable representing discharge, stage, velocity, river width etc. and θ is weight coefficient, where $0\le\theta\le1$.

CASE STUDY

Study area and data

The Qiantang River basin is located at the east part of China (Figure 1), and is famous for the Qiantang tidal bore. The astronomical tides in the Qiantang estuary are of the irregular semi-diurnal kind. The tidal effect can extend upstream to Tonglu in spring tide, about 281 km to the mouth of the Hanzhou Bay (Pan *et al.* 2007). The reach from Tonglu to Fuyang is selected as the study area. Tonglu is the upstream boundary controlled by flood, and Fuyang is the downstream boundary affected by tide. The length from Tonglu to Zhaixi is about 15.6 km, and about 28.6 km from Zhaixi to Fuyang. There are 50 complex cross-sections surveyed from Tonglu to Fuyang, varying with different main channels and floodplains.

Nine flood events from 1986 to 1989 were adopted to simulate the river stages at Zhaixi with the stages at Tonglu and Fuyang. Considering the complexity of the roughness estimation, the roughness values calibrated from the SVN model were adopted in the SVN-1 and -2 models. This choice may affect the model performance, but allows the performance of the SVN, SVN-1 and SVN-2 models to be compared under the same conditions.

Evaluation criteria

Considering that the peak stage value and the peak stage occurrence time of a hydrograph are of the most concern during floods, the peak stage error (PSE), the relative peak stage error (RPSE) and the peak stage timing error (PTE) are calculated. PSE < 0 and RPSE < 0 imply that the stage simulated is larger than the observed, and vice versa. PTE < 0 means that the calculated peak stage occurs after the observed, and vice versa. Additionally, the root mean square error (RMSE) is employed to evaluate the residual between observed and forecast water stages, and the Nash–Sutcliffe coefficient (CE) is used to evaluate the simulation performance between observed and simulated stage hydrographs. The expressions of RMSE and CE (Nash & Sutcliffe 1970) are as follows:

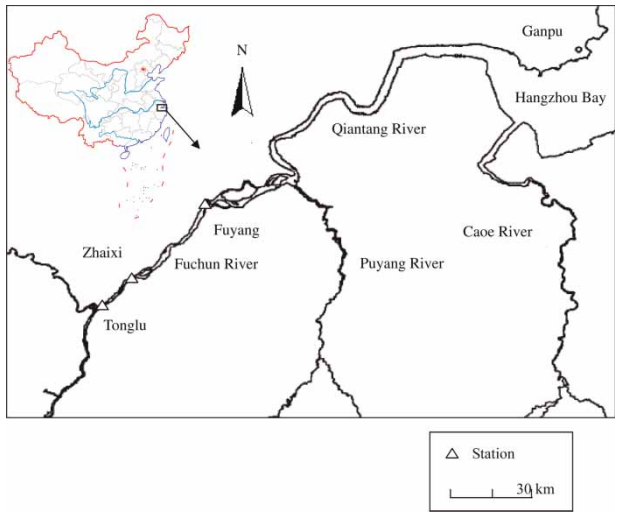

Figure 1 | Location of the study site.

$$\mathrm{RMSE} = \sqrt{\frac{\sum_{i=1}^{n} [\mathrm{Obs}\, Z(i) - \mathrm{Cal}\, Z(i)]^2}{n}} \tag{6}$$

and

$$\mathrm{CE} = 1 - \frac{\sum_{i}^{n} [\mathrm{Cal}\, Z(i) - \mathrm{Obs}\, Z(i)]^2}{\sum_{i=1}^{n} [\mathrm{Obs}\, Z(i) - \overline{\mathrm{Obs}\, Z}]^2} \tag{7}$$

where $\mathrm{Obs}\, Z(i)$ and $\mathrm{Cal}\, Z(i)$ represent the observed stage and calculated stage at the time of i, respectively, $\overline{\mathrm{Obs}\, Z}$ is the average observed stage and n is the number of the observations.

Model calibration

The α coefficient is the only parameter which needs to be estimated in the tidal effect expressions. The initial values of the α coefficient are obtained by using the trial-and-error method. The minimization of the sum of squares of the residuals between the observed stages and simulated stages is used as the objective function to optimize the α coefficient in this study. The simulation results at Zhaixi in the Qiantang River by using the SVN model are listed in Table 1. Results from the SVN-1 and -2 models with the optimized values of α are listed in the columns entitled (1) and

Table 1 | Results of simulation at Zhaixi in the Qiantang River with SVN model

Flood event	Start time	End time	PSE (m)	RPSE (%)	PTE (h)	RMSE (m)	CE
860501	1986-05-01 08	1986-05-07 08	–0.29	–3.3	0	0.203	0.925
860617	1986-06-17 09	1986-06-29 08	–0.30	–3.6	0	0.278	0.812
860705	1986-07-05 08	1986-07-11 08	–0.30	–3.7	1	0.429	0.694
870620	1987-06-20 00	1987-06-28 00	–0.73	–6.4	0	0.549	0.895
870722	1987-07-22 05	1987-08-02 02	–0.99	–9.4	1	0.508	0.845
880511	1988-05-11 11	1988-05-16 01	–0.70	–7.1	–1	0.553	0.786
880616	1988-06-16 00	1988-06-26 00	–0.78	–6.5	2	0.510	0.898
890527	1989-05-27 10	1989-06-06 06	–0.84	–7.3	0	0.726	0.824
890616	1989-06-16 01	1989-06-26 00	–0.75	–6.9	1	0.477	0.879

Table 2 | Results of simulation at Zhaixi in the Qiantang River with optimized α

Flood event	PSE (m)		RPSE (%)		PTE (h)		RMSE (m)		CE		α	
	(1)	(2)	(1)	(2)	(1)	(2)	(1)	(2)	(1)	(2)	(1)	(2)
860501	–0.24	–0.32	–2.7	–3.6	–2	0	0.180	0.202	0.941	0.925	38	19
860617	–0.30	–0.59	–3.6	–7.0	0	–2	0.258	0.268	0.839	0.826	28	32
860705	–0.20	–0.34	–2.4	–4.2	1	1	0.417	0.425	0.711	0.700	33	27
870620	–0.89	–0.71	–7.7	–6.2	1	–1	0.522	0.486	0.905	0.918	10	29
870722	–0.21	–0.66	–2.0	–6.3	–4	1	0.469	0.494	0.868	0.854	21	19
880511	–0.55	–0.65	–5.5	–6.5	–3	0	0.523	0.539	0.809	0.797	27	27
880616	–0.32	–0.70	–2.7	–5.9	–3	5	0.392	0.490	0.939	0.906	36	15
890527	–1.28	–0.77	–11.1	–6.7	–2	5	0.609	0.659	0.876	0.855	32	27
890616	–0.97	–0.71	–8.9	–6.5	0	0	0.402	0.438	0.914	0.898	27	18

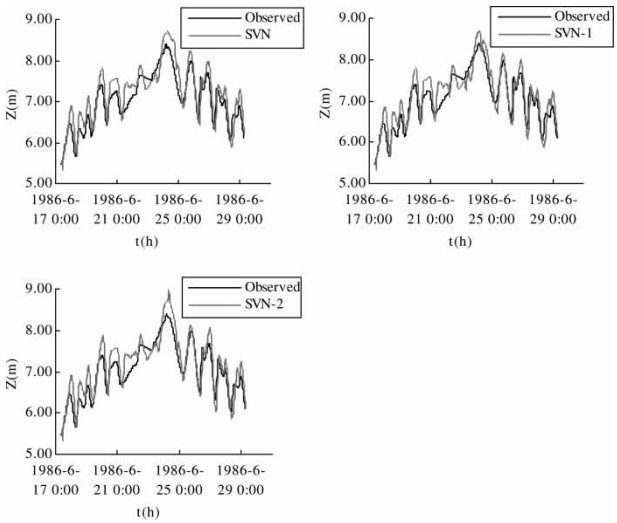

Figure 2 | Stage hydrograph of flood 860617 at Zhaixi in the Qiantang River.

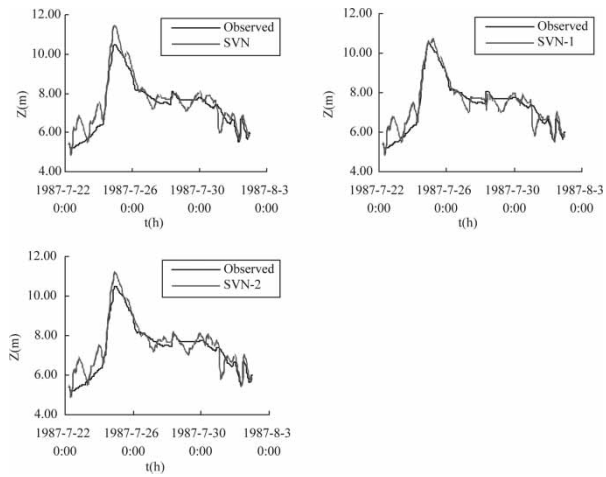

Figure 3 | Stage hydrograph of flood 870722 at Zhaixi in the Qiantang River.

(2), respectively, in Table 2. Some selected hydrographs are shown in Figures 2 and 3.

As shown in Tables 1 and 2, the performances of the SVN-1 and -2 models are better than that of the original SVN model. The CE values of these flood events using the SVN-1 model and eight flood events (except 860501) using the SVN-2 model are larger than those obtained using the original SVN model. The RMSE values of these flood events with the SVN-1 and -2 models are all lower than those obtained with the SVN model. The PSE of five flood events with the SVN-1 model and six flood events with the SVN-2 model are smaller than those obtained with the SVN model. From Figures 2 and 3, it can be seen that the hydrographs calculated by the SVN-1 and -2 models have better agreement with the observed data than that of the SVN model. In particular, the SVN-1 and -2 models can describe water-level fluctuation due to tidal effect both in the rising limbs and recession limbs. It demonstrates that the tidal effect expressions considered in the SVN-1 and -2 models are reasonable for representing the river stage fluctuation caused by tidal effect.

From Table 2, the CE values from the SVN-1 model (except 870620) are higher than that from the SVN-2 model, and the RMSE values from the SVN-1 model (except flood 870620) are lower than that from the SVN-2 model. Moreover, the reduction in the PSE for the SVN-1 model is larger than that for the SVN-2 model; for instance, the PSE of flood 870722 reduces from –0.99 m to –0.21 m for SVN-1 and to –0.66 m for SVN-2. From Figures 2 and 3, the agreements between the observed and calculated data using the SVN-1 model are better than those obtained from the SVN-2 model. It is clear that the SVN-1 model performs better than the SVN-2 model, and the expression for tidal effect considered in the SVN-1 model is more effective at accounting for tidal effect.

In order to show the best performance of the SVN-1 and -2 models, the values of α are respectively optimized for each flood in Table 2. For these nine flood events, α has values in the range 10–38 for the SVN-1 model and 15–32 for the SVN-2 model. In practical applications, its value should be calibrated from historical flood events. In this study, these flood events were split into two independent subsets for model calibration and validation respectively: seven flood events (1986–1988) for calibration and two flood events in 1989 for validation. By averaging the optimized value of α for seven flood events from 1986 to 1988, the calibrated value of α was estimated as 28 for the SVN-1 model and 24 for the SVN-2 model.

RESULTS AND DISCUSSION

The results at Zhaixi from the SVN-1 and -2 models with the calibrated α are listed in Table 3, and some selected hydrographs are displayed in Figures 4 and 5. The scatter plots of the observed stages and the simulated stages for calibration and validation with the calibrated α are shown in Figure 6.

By comparing the results of the SVN-1 and -2 models in Table 2 with those in Table 3, we note that there exists little

Table 3 | Results of simulation at Zhaixi in the Qiantang River with calibrated α

Flood event	PSE (m) (1)	(2)	RPSE (%) (1)	(2)	PTE (h) (1)	(2)	RMSE (m) (1)	(2)	CE (1)	(2)
860501	–0.25	–0.33	–2.9	–3.7	–2	0	0.182	0.202	0.939	0.925
860617	–0.30	–0.53	–3.6	–6.3	0	–2	0.258	0.269	0.839	0.824
860705	–0.22	–0.34	–2.7	–4.2	1	1	0.417	0.425	0.710	0.699
870620	–1.01	–0.71	–8.8	–6.2	–3	–1	0.418	0.496	0.939	0.914
870722	0.09	–0.60	0.8	–5.7	–4	1	0.483	0.503	0.860	0.848
880511	–0.53	–0.65	–5.4	–6.6	–3	0	0.523	0.540	0.809	0.797
880616	–0.57	–0.73	–4.8	–6.1	–3	6	0.410	0.470	0.934	0.913
890527	–1.27	–0.78	–11.0	–6.8	–1	5	0.613	0.662	0.875	0.854
890616	–0.97	–0.96	–0.72	–6.6	–1	0	0.402	0.457	0.914	0.888

difference in the evaluation indices of these simulated results with the optimized and calibrated α; this factor indicates that the calibrated value of α is reasonable. As shown in Tables 1 and 3, the CE values are all greater for the SVN-1 and -2 models in comparison with those from the SVN, and the CE values from the SVN-1 model are higher than those from the SVN-2 model. The maximum increase in CE for the SVN model is from 0.824 to 0.875 for the SVN-1 model for flood 890527.

The RMSE values are all reduced for the SVN-1 and -2 models in comparison with those from the SVN model, and the RMSE values from the SVN-1 model are lower than those from the SVN-2 model. The maximum decrease in RMSE for the SVN model is from 0.549 to 0.418 for the SVN-1 model for flood 870620. The errors in peak stages for the SVN-1 model (except flood 870620, 890527 and 890616) are lower than those for the SVN-2 model. The maximum error in RPSE is –9.4% for flood 870722 for the SVN model, –0.8% for the SVN-1 model and –5.7% for the SVN-2 model. The errors in the peak stage occurrence time for the SVN-1 model are not more than 3 hours, while the errors are more than 3 hours with the SVN-2 model for floods 880616 and 890527.

Figures 4 and 5 show that the agreements between the observations and calculations when using the SVN-1 and -2 models with the calibrated α are all better than these for the original SVN model; moreover, the agreements for the

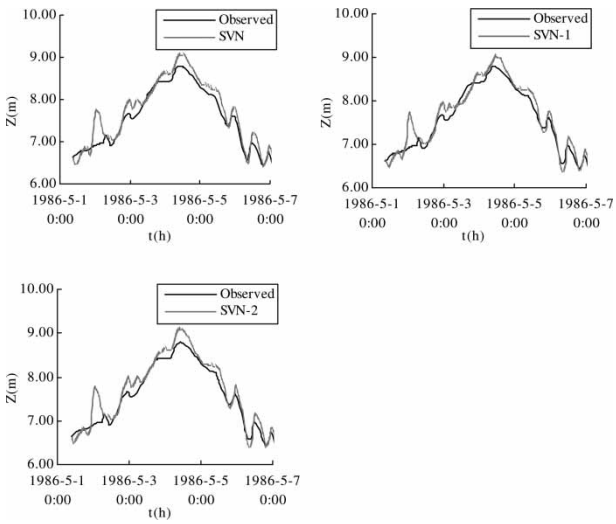

Figure 4 | Stage hydrograph of flood 860501 at Zhaixi in the Qiantang River.

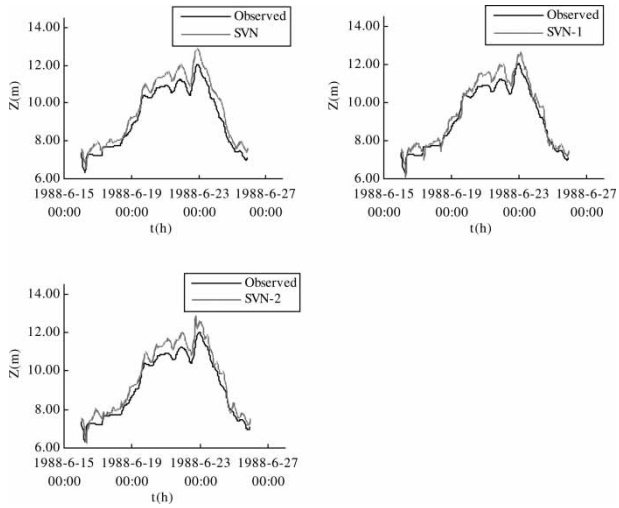

Figure 5 | Stage hydrograph of flood 880616 at Zhaixi in the Qiantang River.

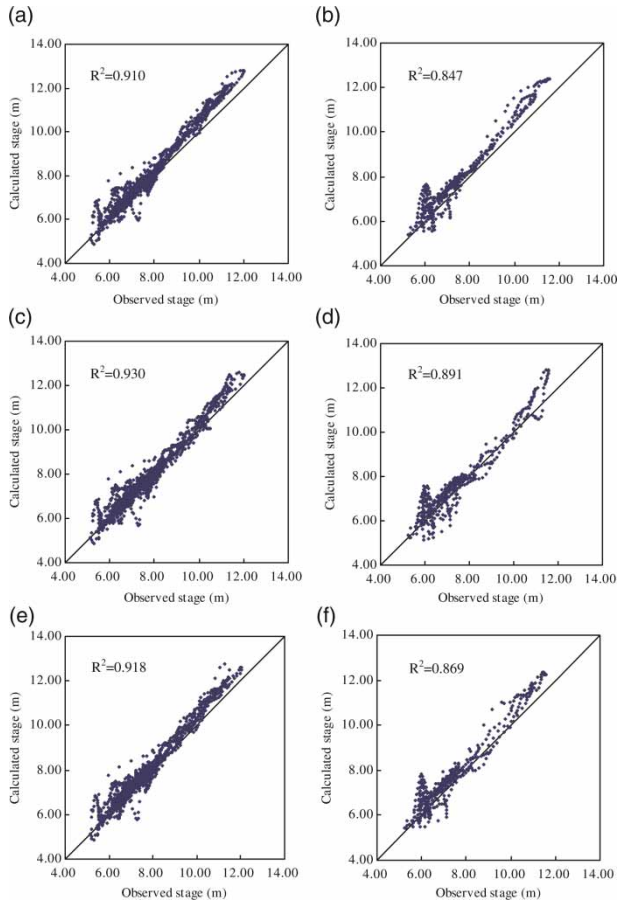

Figure 6 | Comparison of observed and calculated stages with calibrated α at Zhaixi in the Qiantang River: (a) calibration results with SVN model; (b) validation results with SVN model; (c) calibration results with SVN-1 model; (d) validation results with SVN-1 model; (e) calibration results with SVN-2 model; and (f) validation results with SVN-2 model.

SVN-1 model are better than those for the SVN-2 model. From Figure 6, it is clear that the simulations using the SVN-1 model correlated better with the observations than those for the SVN-2 and SVN models (both in model calibration and validation). The correlation coefficients for the calibration and verification results are 0.930 and 0.891, respectively, for the SVN-1 model; 0.918 and 0.869 for the SVN-2 model; and 0.910 and 0.847 for the SVN model. Moreover, it can be seen that the SVN-1 model can simulate high river stages more accurately than the SVN-2 and SVN models.

From the analysis above, the results of the SVN-1 and -2 models with the calibrated α are better than those obtained from the SVN model (except PTE for some flood events), and the SVN-1 model performs better than the SVN-2 model. It can be concluded that the SVN-1 model with calibrated α can be used for tidal river stage forecasting. It also indicates that the expression developed for the SVN-1 model is reasonable, and can effectively reflect the tidal effect on flood routing in tidal rivers.

Why is the performance of the SVN-1 model better than the SVN-2 model in the tidal channel of the Qiantang River? From the expressions $\alpha(B_T/B_x)\omega|(\partial T/\partial t)|$ and $\alpha(B_T/B_x)|\omega|(\partial T/\partial t)$, the former uses the wave velocity ω to control the tidal effect direction while the latter adopts the tidal level change rate at the downstream boundary, namely $(\partial T/\partial t)$, to represent the direction. In tide propagation, tidal flow has different directions at different phases of the tide cycle. At the beginning of the process from ebb to flood, the direction of tidal flow at the channel mouth is downstream and then upstream; at the beginning of the process from flood to ebb, the flow direction is upstream and then downstream. It is clear that the direction of tidal effect is not directly controlled by the process of flood tide or ebb tide. The possible reason is that the tidal velocity has more impact on flood during the transition of propagation direction upstream or downstream than the tidal level change rate. This interpretation needs to be verified from more applications in other tidal rivers.

From Figures 2–5, we note that the simulated peak floods in these stage hydrographs are all higher than those observed. Part of the problem is that the estimated parameter values include the roughness and the α coefficient. It is found that the simulated peak stage can be reduced by adjusting the roughness values in the SVN model. The roughness values for the SVN-1 and -2 models are from the SVN model in this study, resulting in the same problem. The estimated roughness values only reflect mean condition; however, it is known that the roughness varies with flow and channel geometry. Roughness correction methods can be considered (e.g. Hsu *et al.* 2006; Bao *et al.* 2009), which is beyond the scope of this paper. It is also found that the agreement in the peak floods can be improved by tuning the α value. In the model calibration, the sum of squares of the residuals between the observations and simulations is used as the objective function. Some other objective functions, such as PSE as well as multi-objective function, can be considered in a further study. More work on parameter analysis is needed.

It can also be found that the error in the peak stage occurrence time from the SVN-1 and -2 models is larger than that from the SVN model for some flood events, which indicates that the SVN-1 and -2 models have no capacity for improving the accuracy of the peak stage occurrence time in comparison with the SVN model. Part of the reason is that the tide propagation time from the downstream boundary to a specific section is not considered in the developed expressions, which only use the tidal level change rate at time t to reflect the tidal effect on flood at the section at the same time. One possible method considering the tide propagation time is to use the change rate of the tidal level at time $t-t_x$ to reflect the tidal effect on flood at time t at a specific section (t_x is the time taken for tide to travel from the downstream boundary to the section). Considering that tide propagation time varies under different flow conditions, its average value for a specific section can be employed. More analysis is needed in this aspect. For the sake of safety, we should compare the peak stage occurrence time calculated by the SVN-1 model with that by the SVN model. If there is a large difference between them, the forecast hydrographs should be analysed in detail.

CONCLUSIONS

In terms of the characteristics of tide propagation along a tidal channel, two expressions were conceptually

developed to represent the comprehensive effect on flood routing caused by the tide including the channel geometry, the tidal wave velocity and the change rate of tidal level at the downstream boundary. These expressions can be directly added to the SVN model based on the standard Saint-Venant equations to establish the SVN-1 and -2 models. The case study in the tidal reach of the Qiantang River shows that the SVN-1 model can obtain satisfactory accuracy in comparison with the SVN and SVN-2 models. It is concluded that the expression employed in the SVN-1 model can effectively reflect tidal effect, and the SVN-1 model can improve river stage forecasting in tidal rivers. All of these results should be validated in a wide variety of tidal river systems with more flood events.

The approach of developing conceptual expressions accounting for comprehensive tidal effect adopted here provides an effective and simple way to study the tidal effect on flood routing. We can extend this idea to improve the approach with other information affecting tidal effect, such as wind. More effort is needed for further application, for example parameter calibration such as the α coefficient and river roughness and the improvement in the accuracy of peak stage timing. Due to a shortage of data, only large flood events controlled by an upstream flood are calculated in this case study; the performance of the proposed models for small flood events dominated by tide also should be analysed, however. Additionally, the newly proposed expressions accounting for the tidal effect on flood routing are based on a conceptual analysis; further study should focus on the physical dynamic mechanism of the interactions between flood and tide. In future research, we aim to establish a physical expression for tidal effect according to the findings in this paper, which would produce important insights into the complex flood routing processes in tidal rivers.

ACKNOWLEDGEMENTS

The study was supported by the National Key Technologies R&D Program of China during the 11th Five-year Plan Period (No. 2006BAC05B02; No. 2008BAB29B08-02), the Development Program for Changjiang Scholars and Innovation Team (IRT0717) and the Program for the Ministry of Education and State Administration of Foreign Experts Affairs, P.R. China (B08408).

REFERENCES

Bao, W. M., Zhang, X. Q. & Qu, S. M. 2009 Dynamic correction of roughness in the hydrodynamic model. *Journal of Hydrodynamics* **21** (2), 255–263.

Bao, W. M., Zhao, C., Wang, H. & Qu, S. M. 2007 Application of a bi-directional stage routing model in a tidal reach. Methodology in Hydrology. Nanjing, China: IAHS Publication 311, pp. 46–52.

Chang, F. J. & Chen, Y. C. 2003 Estuary water-stage forecasting by using radial basis function neural networks. *Journal of Hydrology* **270**, 158–166.

Ferrick, M. G. 1985 Analysis of river wave types. *Water Resources Research* **21** (2), 209–220.

Horrevoets, A. C., Savenije, H. H. G., Schuurman, J. N. & Graas, S. 2004 The influence of river discharge on tidal damping in alluvial estuaries. *Journal of Hydrology* **294**, 213–228.

Hsu, M. H., Fu, J. C. & Liu, W. C. 2006 Dynamic routing model with real-time roughness updating for flood forecasting. *Journal of Hydraulic Engineering* **132** (6), 605–619.

Lei, Z. Y., Zhang, J. S. & Kong, J. 2009 Numerical simulation of water level under interaction between runoff and estuarine dynamic in tidal reach of the Yangtze River. *China Ocean Engineering* **23** (3), 543–551.

Liu, W. C., Hsu, M. H. & Kuo, A. Y. 2007 Three-dimensional hydrodynamic and salinity transport modelling of Danshuei River estuarine system and adjacent coastal sea, Taiwan. *Hydrological Processes* **21**, 3057–3071.

Nash, J. E. & Sutcliffe, J. V. 1970 River flow forecasting through conceptual models, 1. A discussion of principles. *Journal of Hydrology* **10** (3), 282–290.

Pan, C. H., Lin, B. Y. & Mao, X. Z. 2007 Case study: numerical modeling of the tidal bore on the Qiantang River, China. *Hydraulic Engineering* **133** (2), 130–138.

Phillips, J. D. & Slattery, M. C. 2007 Downstream trends in discharge, slope, and stream power in a lower coastal plain river. *Journal of Hydrology* **334**, 290–303.

Price, R. K. 2009 An optimized routing model for flood forecasting. *Water Resources Research* **45**, W02426.

Qu, S. M., Bao, W. M., Shi, P., Yu, Z. B. & Jiang, P. 2009 Water-stage forecasting in a multitributary tidal river using a bidirectional Muskingum method. *Journal of Hydrologic Engineering* **14** (12), 1299–1308.

Saavedra, I., López, J. L. & García-Martínez, R. 2003 Dynamic wave study of flow in tidal channel system of San Juan River. *Journal of Hydraulic Engineering* **129** (7), 519–526.

Su, M. D., Xu, X., Zhu, J. L. & Hon, Y. C. 2001 Numerical simulation of tidal bore in Hangzhou Gulf and

Qiantangjiang. *International Journal for Numerical Methods in Fluids* **36** (2), 205–247.

Tayefi, V., Lane, S. N., Hardy, R. J. & Yu, D. 2007 A comparison of one- and two-dimensional approaches to modelling flood inundation over complex upland floodplains. *Hydrological Processes* **21**, 3190–3202.

Tsai, C. W. 2003 Applicability of kinematic, koninertia, and quasi-steady dynamic wave models to unsteady flow routing. *Journal of Hydraulic Engineering* **129** (8), 613–627.

Tsai, C. W. 2005 Flood routing in mild-sloped rivers – wave characteristics and downstream backwater effect. *Journal of Hydrology* **308**, 151–167.

Yu, P. S., Chen, S. T. & Chang, I. F. 2006 Support vector regression for real-time flood stage forecasting. *Journal of Hydrology* **328**, 704–716.

First received 3 October 2009; accepted in revised form 30 July 2010. Available online December 2011